The Ising model on hyperlattices

1992 J. Phys. A: Math. Gen. 25 6577

(http://iopscience.iop.org/0305-4470/25/24/012)

J. Phys. A: Math. Gen. 25 (1992) 6577–6592. Printed in the UK

The Ising model on hyperlattices

Ronald Rietman†, Bernard Nienhuis† and Jaan Oitmaa‡

† Instituut voor Theoretische Fysica, Universiteit van Amsterdam, Valckenierstraat 65, 1018 XE Amsterdam, The Netherlands

‡ School of Physics, The University of New South Wales, Kensington NSW 2033, Australia

Received 16 June 1992

Abstract. We describe the construction of regular lattices in two-dimensional hyperbolic space by means of the action of a discrete subgroup of SU(1,1). We consider an Ising model on such lattices and show how the thermodynamic limit can be handled. We give high- and low-temperature expansions of the free energy, magnetic susceptibility and magnetization and find that these quantities diverge at a critical temperature with mean-field exponents $\beta = 1/2$, $\gamma = 1$. We also conjecture the long distance behaviour of correlation functions at the critical temperature.

1. Introduction and outline

It is well known that critical behaviour is determined by only a few properties, most notably the dimension of the system and the symmetries of the interaction. Another property that might play a role is the curvature of the space in which the system lives. In order to investigate this we study the Ising model in a space of uniform negative curvature, the Poincaré disk. Since the Ising model in a flat two-dimensional space is exactly solvable in many ways, one might hope that one of these methods can be generalized to this curved space.

In order to define an Ising model we need to have some lattice on which the spins live. We want this lattice to be as regular as possible; every site and every edge connecting neighbouring sites must be equivalent. Also the lattice must be planar, since many methods for solving the Ising model in flat space make explicit use of the planarity of the lattice. These requirements restrict the possible lattices. In flat space only three possibilities remain: the square, triangular and honeycomb lattices. On the Poincaré disk there are infinitely many possibilities. We describe the construction of these lattices in section 2. In section 3 we consider the Ising model on these so-called hyperlattices. We are unable to give an exact solution, hence we turn to high- and low-temperature series expansions in section 4. These expansions indicate that the magnetization and susceptibility become singular with the classical, mean-field exponents $\beta = 1/2$ and $\gamma = 1$, at a critical temperature T_c. It is not very surprising that the critical exponents take on their mean-field values, since a counting argument, given in section 2, shows that the effective dimensionality of the hyperlattices is infinite.

A much more surprising result is the value T_c for a self-dual lattice; it is larger than the self-dual value. This implies that there should be a second critical temperature, dual to T_c, but the low-T expansions of the magnetization and susceptibility do not show this singularity.

Finally, in section 5, we turn to a continuum description of the critical point. We calculate, using techniques from conformal field theory, some correlation functions on the Poincaré disk.

2. Hyperlattices

In this section we describe the construction of regular lattices with equilateral faces for which every lattice point has the same coordination number. These lattices can be embedded in a homogeneous two-dimensional space with constant Ricci curvature. When the curvature is positive, this is the sphere S^2. After Riemann projection $z \equiv x + iy = e^{i\varphi} \tan \frac{1}{2}\theta$ this becomes the plane with metric

$$g_{\mu\nu}(x, y) = \frac{1}{(1 + z\bar{z})^2}\delta_{\mu\nu}. \tag{2.1}$$

When the curvature $R = 0$ we simply have the Euclidean plane with metric

$$g_{\mu\nu}(x, y) = \delta_{\mu\nu}. \tag{2.2}$$

When the curvature is negative we may choose the hyperboloid embedded in (2+1)-dimensional Minkowski space, given by

$$X^2 + Y^2 - Z^2 = -\tfrac{1}{4} \qquad Z \geqslant \tfrac{1}{2}. \tag{2.3}$$

This hyperboloid can be parametrized with coordinates $\psi \in [0, \infty)$, $\varphi \in [0, 2\pi)$:

$$X = \tfrac{1}{2}\sinh\psi\cos\varphi \qquad Y = \tfrac{1}{2}\sinh\psi\sin\varphi \qquad Z = \tfrac{1}{2}\cosh\psi \tag{2.4}$$

and in terms of $z \equiv x + iy = e^{i\varphi}\frac{1}{2}\tanh\psi$ it becomes the circular disk $|z| < 1$ with metric

$$g_{\mu\nu}(x, y) = \frac{1}{(1 - z\bar{z})^2}\delta_{\mu\nu}. \tag{2.5}$$

The geodesics of this metric are circular arcs (in the flat metric) orthogonal to the circle at infinity, $|z| = 1$. The distance between two points P_1 and P_2 is given by

$$d(P_1, P_2) = \operatorname{artanh}\left|\frac{z_1 - z_2}{1 - z_1\bar{z}_2}\right|.$$

One is not restricted to the unit disk; by means of a conformal mapping one can transform to another geometry, e.g. by $z \mapsto i(1+z)/(1-z) \equiv u + iv$ to the upper-half plane $\{(u, v)|v \geqslant 0\}$.

The lattices can be characterized by two integers, both $\geqslant 3$: v, the number of neighbours of each vertex; and f, the number of sides of each face, and denoted as (v, f). It can be embedded in the sphere, plane or hyperboloid when the quantity $(v - 2)(f - 2)$ is smaller than, equal to or larger than four.

The five lattices on the sphere correspond to the five platonic solids, e.g. the $(3,3)$ lattice is a tetrahedron and the $(5,3)$ lattice is an icosahedron. They have a finite number of points.

On the plane there are three infinitely large lattices: triangular $(6,3)$, square $(4,4)$ and hexagonal $(3,6)$; and there are many examples of exactly soluble statistical mechanical models on these lattices.

The lattices on the hyperboloid—hyperlatices, for short—also have an infinite number of points. An example of a hyperlattice is shown in figure 1. If we define a statistical mechanical model on such a lattice we must be very careful in taking the thermodynamic limit because the thermodynamic limit can be very sensitive to boundary conditions. This is the result of the fact that the boundary of a finite section of the lattice contains a finite fraction of the points of the entire section, just as in a Cayley tree—see e.g. [1]. We discuss this further in the following.

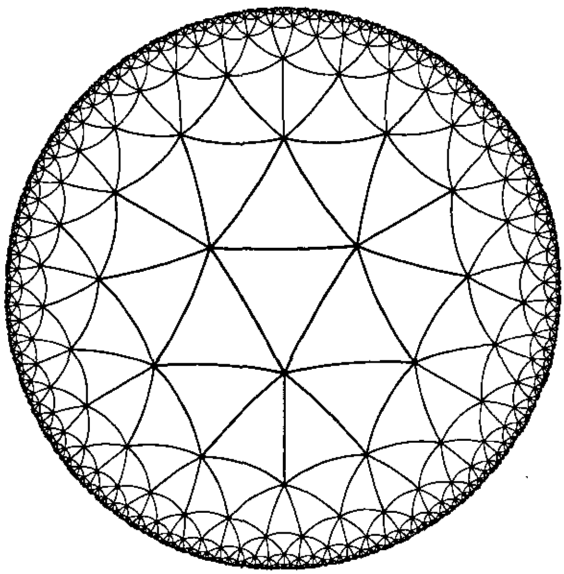

Figure 1. An example of a $(7,3)$ hyperlattice. The bonds are drawn along the geodesics.

We now turn to the construction of the hyperlattices. The description given here is for the unit disk, but it can be easily translated to the hyperboloid or the upper-half plane. The main observation is that the (v,f) lattice has a symmetry group (not taking reflection symmetry into account) that is generated by two elements:

(i) a rotation around a given lattice point over $\alpha = 2\pi/v$;

(ii) a rotation around the centre of an adjacent face over $\beta = 2\pi/f$.

Here 'rotation' and 'centre' are defined with respect to the metric (2.5).

We denote these rotations by a and b respectively and the identity by e. The generators obey the relations

$$a^v = e \tag{2.6}$$

$$b^f = e \tag{2.7}$$

$$(ab)^2 = e. \tag{2.8}$$

The group element ab, being its own inverse, represents a 180° rotation around the centre of an edge.

The group generated by a and b is a subgroup of the group of isometries of the unit disk in the complex plane, the projective group $\mathrm{PSU}(1,1) \equiv \mathrm{SU}(1,1)/\{I,-I\}$. The action of a matrix $M \in \mathrm{SU}(1,1)$ on a point z is given by

$$M(z) = \begin{pmatrix} s & t \\ t^* & s^* \end{pmatrix}(z) = \frac{sz+t}{t^*z+s^*} \qquad |s|^2 - |t|^2 = 1. \tag{2.9}$$

If M has one fixed point inside the circle, i.e. when $|\mathrm{Im}s| > |t|$, it represents a rotation around that fixed point; the rotation angle φ is then given by $2\cos(\varphi/2) = |\mathrm{Tr}M|$.

Since $-M$ has the same action on z as M, they correspond to the same isometry of the unit disk. Such an isometry is therefore represented by two matrices $\pm M \in \mathrm{SU}(1,1)$.

A representation ρ of the symmetry group of the hyperlattice can be easily constructed. Take for example the origin $z=0$ as the given centre of a face and the point $z=r$ ($r \in \mathbb{R}$) as the given adjacent lattice point. Then b can be represented by

$$\rho(b) = \pm \begin{pmatrix} \mathrm{e}^{\mathrm{i}\beta/2} & 0 \\ 0 & \mathrm{e}^{-\mathrm{i}\beta/2} \end{pmatrix} \tag{2.10}$$

and a by

$$\rho(a) = \pm\frac{1}{1-r^2}\begin{pmatrix} \mathrm{e}^{\mathrm{i}\alpha/2} - r^2\mathrm{e}^{-\mathrm{i}\alpha/2} & -r\left(\mathrm{e}^{\mathrm{i}\alpha/2} - \mathrm{e}^{-\mathrm{i}\alpha/2}\right) \\ r\left(\mathrm{e}^{\mathrm{i}\alpha/2} - \mathrm{e}^{-\mathrm{i}\alpha/2}\right) & \mathrm{e}^{-\mathrm{i}\alpha/2} - r^2\mathrm{e}^{\mathrm{i}\alpha/2} \end{pmatrix}. \tag{2.11}$$

Relation (2.8) is satisfied when

$$r^2 = \frac{\cos((\alpha+\beta)/2)}{\cos((\alpha-\beta)/2)}. \tag{2.12}$$

The lattice points are generated by acting with 'words' in a and b on r. Equations (2.6)–(2.8) define an equivalence relation between such words. Equivalent words, when acting on r, give the same lattice point, but since $a(r) = r$ and $a^v = e$, the mapping from equivalence classes of words to lattice points is v to one.

The equivalence classes of words form a group $G(v,f)$ denoted by

$$G(v,f) = \langle a, b;\, a^v = b^f = (ab)^2 = e\rangle. \tag{2.13}$$

The action of two elements g_1 and g_2 of $G(v,f)$ on r gives nearest neighbours on the lattice when $g_2 = g_1 a^n b a^m$ for some $m, n = 0, 1, \ldots, v-1$, since $a^n b(r)$ are the neighbours of r and $a^m(r) = r$. We will connect nearest neighbours by directed bonds that carry an arrow. These directed bonds are in 1–1 correspondence with the elements of $G(v,f)$.

The hyperlattices are in a sense infinite dimensional. This can be seen as follows. The lattice can be divided in layers in a natural way, see figure 2. The first layer consists of a single (central) face and the bonds and sites adjacent to it, or, alternatively, of the v faces meeting at a (central) site and the bonds and sites adjacent to it. The central site itself may be viewed as the zeroth layer. The second

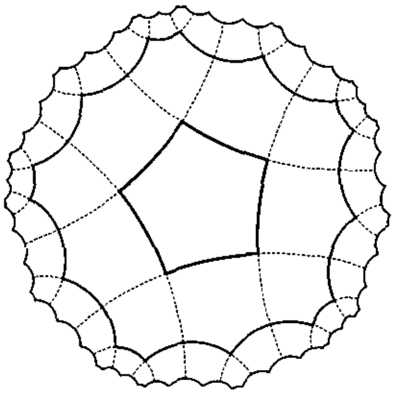

Figure 2. The division in layers for a (4,5) lattice. The sites within the first, second and third layer are connected by solid bonds, the bonds between consecutive layers are broken.

layer consists of those faces that have a site in common with the first layer and the bonds and sites adjacent to these faces that do not belong to the first layer. The third, fourth, etc layers are formed in a similar way.

It is easy to derive recursion relations for the number of sites, edges and faces in each layer. We give the derivation for the sites, the derivations for the edges and the faces can be done in a similar way. We first consider the case $f \geqslant 4$. Within each layer the sites can be divided into two classes: the ones that are connected to the previous (inner) layer and those that are not. We denote the number of these points in the nth layer by I_n and E_n respectively. The number of points in the nth layer is $I_n + E_n$ and the following recursion relation is satisfied:

$$\begin{pmatrix} I_{n+1} \\ E_{n+1} \end{pmatrix} = \begin{pmatrix} v-3 & v-2 \\ fv-3f-3v+8 & fv-2f-3v+5 \end{pmatrix} \begin{pmatrix} I_n \\ E_n \end{pmatrix} \tag{2.14}$$

with initial condition $I_1 = 0$, $E_1 = f$ (for the 'face-centred' lattice) or $I_1 = v$, $E_1 = v(f-3)$ (for the 'site-centred' lattice). So the number of points in the nth layer grows as

$$I_n + E_n \sim \lambda_{\max}^n$$

with

$$\lambda_{\max} = \tfrac{1}{2}(f-2)(v-2) - 1 + \left\{\left(\tfrac{1}{2}(f-2)(v-2) - 1\right)^2 - 1\right\}^{1/2}. \tag{2.15}$$

For $f = 3$ the situation is different; for all layers but the first the points fall into two classes: those that are connected to two points of the previous layer and those that are connected to only one point of the previous layer. Denoting the number of these points by I_n and E_n we find the following recursion relation:

$$\begin{pmatrix} I_{n+1} \\ E_{n+1} \end{pmatrix} = \begin{pmatrix} 1 & 1 \\ v-6 & v-5 \end{pmatrix} \begin{pmatrix} I_n \\ E_n \end{pmatrix} \qquad n \geqslant 2 \tag{2.16}$$

with initial condition $I_2 = 3$, $E_2 = 3v - 12$ (for the 'face-centred' lattice) or $I_1 = 0$, $E_1 = v$ (for the 'site-centred' lattice). So in this case the number of points also grows exponentially for the hyperlattices ($v \geqslant 7$).

Thus we see that for a section of the lattice consisting of the first n layers, V_n, the number of points on the boundary, $|\partial V_n|$, is proportional to $|V_n|$. For an 'ordinary' lattice in d dimensions the relation is $|\partial V_n| \sim |V_n|^{1-1/d}$ and therefore it is natural to take $d = \infty$ for the hyperlattices. In this sense the hyperlattices are similar to Cayley trees, where a finite fraction of the points also lies on the boundary. The Cayley trees may be viewed as $f = \infty$ hyperlattices.

3. The Ising model on hyperlattices

The Ising model on these hyperlattices has been considered by previous authors [2, 3]. The main theorem of [3] is that for low temperatures there exist uncountably many Gibbs states. These Gibbs states are characterized by a geodesic and the condition that the boundary spins have the value $+1$ on one side of the geodesic and -1 on the other. Again this is reminiscent of the situation on the Cayley tree, since there the translation symmetry can be broken by fixing the boundary spins to be $+1$ on one side of a line joining two points on the boundary and -1 on the other side.

We will first consider the Ising model at high temperatures on a finite section of the lattice with free boundary conditions. The Hamiltonian is

$$-\beta\mathcal{H}(\{s\}) = K\sum_{(i,j)} s_i s_j + H\sum_i s_i \tag{3.1}$$

and, using standard arguments, the partition function for zero magnetic field can be rewritten as a sum over all possible configurations of diagrams with all vertices of even degree embedded in the lattice

$$Z_{\text{free}}(v, f, K) = \sum_{\{s\}} \mathrm{e}^{-\beta\mathcal{H}(\{s\})} = 2^{N_s}(\cosh K)^{N_e} \sum_{\text{diagrams}} (\tanh K)^L \tag{3.2}$$

where N_s is the number of sites, N_e is the number of edges and L is the total number of edges occupied by the diagrams. The diagram summation starts as follows

$$\sum_{\text{diagrams}} (\tanh K)^L = 1 + N_f(\tanh K)^f + N_{f\text{-}f}(\tanh K)^{2f-2} + \cdots \tag{3.3}$$

where N_f and $N_{f\text{-}f}$ are the number of f-gons and the number of pairs of f-gons joined by a common edge. For flat lattices, where the fraction of sites near the boundary goes to zero for large sections, the number of edges, sites, f-gons, etc, is proportional to the number of sites, and the constants of proportionality are independent of the precise choice of the sections. (For example for the square lattice $N_e/N_s \to 2$, $N_4/N_s \to 1$, independently of details such as the ratio height/width of the sections and whether or not there are 'dangling bonds' at the boundary.) There is no such property for the hyperlattices because of the finite fraction of sites at the boundary, so, strictly speaking, the thermodynamic limit of the free energy does not exist for these lattices. Similar remarks apply to the graphical expansions of other thermodynamic quantities. One might, however, choose only sections of the hyperlattice such that all ratios N_e/N_s, N_f/N_s etc, go to constant values as $N_s \to \infty$, and obtain a 'restricted' thermodynamic limit, which depends on the treatment of the boundary.

It is possible, as in Euclidean space, to impose periodic boundary conditions, by identifying the boundaries of a finite lattice. Finite periodic hyperlattices are then embedded in a Riemann surface, of a genus proportional to the total area. In such a construction the ratios N_e/N_s and N_f/N_s are independent of the size of the lattice and take the bulk values. However, we have not been able to give a general construction of arbitrarily large lattices with periodic boundary conditions.

We shall follow a slightly different route; we *define* a bulk free energy by means of the previous expansion and by assigning to all ratios N/N_s that occur the value they would have if all sites were internal (i.e. far enough away from the boundary). So we take the view that all sites of our lattice are equivalent. In this sense the thermodynamic functions we define represent local bulk properties in a region far removed from the boundaries. So, for example, the ratio N_e/N_s is set equal to $v/2$, since all internal sites are connected to v neighbours and every edge connects two sites.

All differences between this bulk free energy and the free energy in a restricted thermodynamic limit can be attributed to the boundary. For instance, on a Cayley tree $N_e = N_s - 1$, independent of the coordination number v, so the free energy per site is

$$-\beta f_{\text{Cayley}} = \log 2 + \log\cosh K \tag{3.4}$$

whereas the bulk free energy per site, as defined above, is given by

$$-\beta f_{\text{bulk, Cayley}} = \log 2 + \tfrac{1}{2} v \log\cosh K. \tag{3.5}$$

The difference between f and f_{bulk} is the boundary free energy.

The free energy thus defined can be rewritten in a form that reflects the lattice structure by means of a matrix W, first introduced for the square lattice by Vdovichenko [4]:

$$\sum_{\text{diagrams}} x^L = \exp\left(\tfrac{1}{2}\mathrm{Tr}\log(1 - \mathrm{xW})\right). \tag{3.6}$$

The rows and columns of W are labelled by the directed bonds of the lattice. The matrix W generates the steps from one directed bond to another that a random walker can make and it assigns a factor $(-1)^{1+n}$ to a loop with n self-intersections. For the three 'flat' lattices the right-hand side of (3.5) can be evaluated directly, using the translation invariance of these lattices.

As noted in the previous section, there is a one-to-one correspondence between directed bonds and the elements of the group $G(v,f)$, once a particular edge is chosen as the identity e. Choosing e relative to the rotations a and b as in figure 3, a random walker, who is at the directed bond labelled by g at time t and takes one step per unit of time, is at one of the $v-1$ directed bonds labelled by $ga^2b, ga^3b, \ldots, ga^vb$ at time $t+1$ since the edges that can be reached from e are a^2b, $a^3b, \ldots, a^vb$, as shown in figure 3. When g is is near the boundary of the section, the walker can

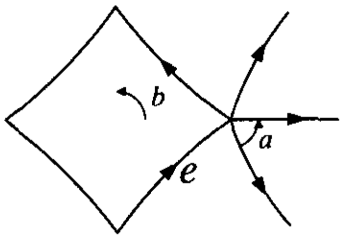

Figure 3. The directed bonds that can be reached from e on a $(5,4)$ hyperlattice. They correspond to the group elements a^2b, a^3b, a^4b and $a^5b = b$, in counterclockwise order.

reach fewer bonds, but we can ignore this complication for the calculation of the bulk free energy.

The matrix W acts on a vector space $V(v, f)$ spanned by basis vectors labelled by the group elements of $G(v, f)$. We define an inner product such that these basis vectors are orthonormal:

$$\langle g_1|g_2\rangle = \delta(g_1, g_2) = \begin{cases} 1 & \text{if } g_1 = g_2 \\ 0 & \text{if } g_1 \neq g_2. \end{cases} \tag{3.7}$$

We then define linear operators A and B on $V(v, f)$ with the properties

$$\langle g_1|A|g_2\rangle = 0 \qquad \text{unless } g_2 = g_1 a \tag{3.8}$$

$$\langle g_1|B|g_2\rangle = 0 \qquad \text{unless } g_2 = g_1 b \tag{3.9}$$

$$A^v = -1 \tag{3.10}$$

$$B^f = -1 \tag{3.11}$$

$$(AB)^2 = -1. \tag{3.12}$$

In terms of these operators W is given by

$$W = -A^2B - A^3B - \cdots - A^vB. \tag{3.13}$$

There is some freedom in the choice of minus signs in these formulae, but this is the simplest choice (in that the signs do not depend on v or f). That W as defined earlier gives every loop the correct sign $(-1)^{1+n}$ can be shown by induction; first one checks that the loops that surround a single face get the correct sign (-1), then one checks that the sign remains correct if a loop is enlarged by surrounding one more face.

If S is any word in the letters A and B, then

$$\mathrm{Tr}S = \begin{cases} 2N_e & \text{if } S = 1 \\ -2N_e & \text{if } S = -1 \\ 0 & \text{otherwise.} \end{cases} \tag{3.14}$$

So on expanding the logarithm in (3.6) and taking the trace one gets

$$-\beta f_{\text{free}} = \log 2 + \frac{v}{2}\log\cosh K - \frac{v}{2}\sum_{\ell=1}^{\infty}\frac{(-\tanh K)^\ell}{\ell}(n_\ell(1) - n_\ell(-1)) \tag{3.15}$$

where $n_\ell(\pm 1)$ is the number of words consisting of ℓ syllables from the set $\{A^2B, A^3B, \ldots, A^vB\}$ that are equal to ± 1.

This result is very nice, but unfortunately it is not very useful for actually computing the free energy, since the word problem for the group

$$\overline{G}(v, f) = \langle A, B; A^v = B^f = (AB)^2 = -1 \rangle$$

is too difficult. Furthermore, other thermodynamic quantities, such as the susceptibility, do not have such a nice representation in terms of the group $\overline{G}(v, f)$. So for practical purposes it is better to enumerate the graphs directly.

A similar word problem for the modular group can be solved. This allowed Lund *et al* [5] to obtain the free energy for the Ising model on the corresponding lattice, which also has a natural embedding in the hyperplane.

At this point it is necessary to make a remark about duality and the free energy expansion at low temperature. The standard Kramers–Wannier duality is established by noting that the diagrams in the high-T expansion correspond to contours that separate regions of up and down spins in a low-T expansion of an Ising model on the dual lattice, at the dual temperature given by

$$\mathrm{e}^{-2\tilde{K}} = \tanh K. \tag{3.16}$$

The dual lattice is obtained by first removing all dangling bonds at the boundary of the original lattice (these bonds cannot be part of a diagram), then putting dual sites at all faces of the amputated lattice, including the external face 'at infinity', and finally joining the dual sites at adjacent faces by dual bonds. Every edge of the amputated lattice is crossed by precisely one dual bond. In order to embed this dual lattice in a hyperlattice with $(\tilde{v}, \tilde{f}) = (f, v)$ one replaces the dual site at infinity by as many sites as there are edges at the boundary of the amputated original lattice. These sites are the boundary sites of the new dual lattice.

The partition function for the Ising model with coupling constant $\tilde{K}$ in zero field on this dual lattice, with the boundary condition that all spins at the boundary are fixed at the same value is given by

$$Z_{\text{fixed}}(f, v, \tilde{K}) = \mathrm{e}^{\tilde{N}_{\ell}\tilde{K}} \sum_{\text{contours}} \left(\mathrm{e}^{-2\tilde{K}}\right)^{L}. \tag{3.17}$$

Using (3.16), the sum over contours becomes identical to the sum over diagrams in (3.2). This allows us to define a bulk free energy per site on a (f, v) lattice for fixed boundary conditions in terms of the bulk free energy per site on a (v, f) lattice with free boundary conditions:

$$-\beta f_{\text{fixed}}(f, v, \tilde{K}) = -\beta \frac{f}{v} f_{\text{free}}(v, f, K) + \frac{f}{2}K - \frac{f}{v}\log 2 - \frac{f}{2}\log\cosh K. \tag{3.18}$$

For the square lattice $f = v = 4$ and one can show that the bulk free energy is independent of the boundary conditions. In that case (3.18) implies that if there is only one critical temperature, it should be at the value K_c for which $\tilde{K}_c = K_c$, i.e. at $K_c = K_{\text{self-dual}} = \frac{1}{2}\log(1 + \sqrt{2})$. However, for hyperlattices there is no reason to assume that $f_{\text{fixed}} = f_{\text{free}}$ and hence one cannot conclude that for lattices with

$f = v \geqslant 5$ there is a critical point at $K = K_{\text{self-dual}}$. But one can conclude from (3.18) the following relation between the critical temperatures of the Ising model with free and with fixed boundaries:

$$\tanh K_{\mathrm{c\,free}}(v, f) = \mathrm{e}^{-2K_{\mathrm{c\,fixed}}(f,v)}. \tag{3.19}$$

In the next section this relation is tested by means of exact series expansions of the magnetic susceptibility (high T) and magnetization (low T) for a self-dual $(5,5)$ lattice.

4. Series expansions

In this section we investigate the Ising model on the $(v, f) = (7,3)$ and $(5,5)$ hyperlattices by the method of exact series expansions [6]. This approach has been highly successful in the past for the standard lattices and there is no difficulty in extending the method to the present cases.

High-temperature expansions for the bulk free energy and zero-field susceptibility (with free boundary conditions) can be developed in the form

$$-\beta f_{\text{free}} = \log 2 + \frac{v}{2} \log\cosh K + \sum_n a_n x^n \tag{4.1}$$

and

$$\chi_{\text{free}} = 1 + \sum_n b_n x^n \tag{4.2}$$

where $x = \tanh K$. The coefficients a_n, b_n are sums of the embedding factors for certain classes of diagrams on the lattice; a_n results from diagrams with n edges and all vertices of even degree, while b_n results from diagrams with n edges and exactly two vertices of odd degree. In practice it is possible to eliminate the disconnected diagrams [7] and we have used this approach here. In table 1 we give the expansion coefficients for the free energy (to 14 terms) and for the susceptibility (to 11 terms) for the two lattices. As is usual for high-T series the susceptibility series is quite regular and amenable to successful analysis, while the free energy coefficients are much more erratic. This is particularly true for the $(5,5)$ lattice.

It is also useful to develop series which converge at low temperature. This consists of enumerating low-energy configurations perturbed from the ferromagnetic ground state, corresponding to fixed boundary conditions, and gives an expansion of the form

$$-\beta f_{\text{fixed}} = \tfrac{1}{2} vK + H + \sum_r L_r(u)\mu^r \tag{4.3}$$

where H is an applied magnetic field and the variables u and μ are given by

$$u = \mathrm{e}^{-2K} \qquad \mu = \mathrm{e}^{-2H}.$$

From this result we obtain expressions for the magnetization and low-temperature susceptibility in the form

$$M_{\text{fixed}}(u) = 1 + \sum_n c_n u^n \tag{4.4}$$

$$\chi_{\text{fixed}}(u) = \sum_n d_n u^n. \tag{4.5}$$

Table 1. Coefficients of the high temperature series for the free energy and susceptibility expansions for the (7,3) and the (5,5) lattices.

	(7,3)		(5,5)	
n	a_n	b_n	a_n	b_n
1	0	7	0	5
2	0	42	0	20
3	$2\frac{1}{3}$	238	0	80
4	$3\frac{1}{2}$	1316	0	320
5	7	7196	1	1270
6	$11\frac{2}{3}$	39 144	0	5040
7	22	212 394	0	20 010
8	$43\frac{3}{4}$	1 150 968	$2\frac{1}{2}$	79 400
9	$94\frac{1}{9}$	6 233 150	0	315 060
10	$206\frac{1}{2}$	33 745 698	−3	1 250 260
11	462	182 669 074	10	4 961 180
12	$1051\frac{1}{6}$		0	
13	2429		−25	
14	$5670\frac{1}{2}$		50	

Table 2 gives the coefficients of these two series for the $(7,3)$ and $(5,5)$ lattices. As is evident the low-T series, while longer, are considerably more erratic than the high-T series—again a well known feature.

We now turn to the analysis, using the standard procedure of ratio plots and Padé approximants [8]. If a function $f(x)$ has an algebraic singularity of the form

$$f(x) \sim A(x_c - x)^{-\gamma} \tag{4.6}$$

then the ratio of successive coefficients has the form

$$r_n \equiv \frac{a_n}{a_{n-1}} = \frac{1}{x_c}\left[1 + \frac{\gamma - 1}{n} + \mathrm{O}\left(\frac{1}{n^2}\right)\right]. \tag{4.7}$$

Hence a 'ratio plot' of r_n against $1/n$ should, for large enough n, become linear with intercept $1/x_c$ and slope $(\gamma - 1)/x_c$.

In figure 4 we show such a plot for the high-T susceptibility series for the $(7,3)$ lattice. Two things are clear. First the points lie on a smooth curve and an extrapolation to $1/n = 0$ is clearly possible with a fair degree of confidence. Second the plot has a definite residual curvature unlike the ratio plots for regular lattices. This is an indication that the exponent $\gamma = 1$, for then the linear term in (4.7) vanishes. This suggests a plot of r_n against $1/n^2$, which is also shown in figure 4. The curvature is reduced, but not eliminated, suggesting that higher order terms are still important. A more sophisticated analysis can be performed, but these results are consistent with a critical point

$$x_c = 0.1848 \qquad K_c = 0.1870$$

and an exponent $\gamma = 1.0$.

The other major approach is the method of Padé approximants, in which the available coefficients of the series are represented by a ratio of polynomials

$$f(x) = \frac{P_L(x)}{Q_M(x)}$$

Table 2. Coefficients of the low-temperature series for the magnetization and susceptibility expansions for the (7, 3) and the (5, 5) lattices.

	(7,3)		(5,5)	
n	c_n	d_n	c_n	d_n
1	0	0	0	0
2	0	0	0	0
3	0	0	0	0
4	0	0	0	0
5	0	0	−2	4
6	0	0	0	0
7	−2	4	0	0
8	0	0	−10	40
9	0	0	0	0
10	0	0	12	−48
11	0	0	−60	360
12	−14	56	0	0
13	0	0	150	−900
14	16	−64	−400	3200
15	−14	84	−102	652
16	0	0	1530	−12 240
17	−84	504	−2800	28 000
18	−28	224	−2100	17 520
19	252	−1512	14 600	−146 000
20	−168	1344	−19 260	234 288
21	−226	1636	−30 260	311 840
22	−224	1792	134 660	−1 615 760
23	−420	4200	−121 310	1 792 140
24	2450	−18 816	−375 130	4 604 279
25	−910	9100	1 207 682	−16 932 396
26	−5068	45 248	−596 000	11 319 680
27	2072	−18 368	−4 276 880	60 930 040
28	−1288	22 192	10 497 200	−169 004 000
29	15 722	−143 108	−483 660	36 375 480
30	1176	−7168	−46 125 332	748 541 168

and singularities in $f(x)$ correspond to zeros of the denominator polynomial $Q_M(x)$ with the residues providing estimates of the exponents. It may be desirable or necessary first to apply transformations to the function, for example by taking the logarithmic derivative [8]. We have carried out such an analysis for the high-T susceptibility series for the (7, 3) lattice, with the result that there is a critical point at $x_c = 0.1848$, consistent with the ratio analysis, and that near x_c $\chi_{\rm free}(x)$ has the approximate representation

$$\chi_{\rm free}(x) = 0.289(x_c - x)^{-1.00} - 1.12. \qquad (4.8)$$

Estimated errors are ± 1 in the last significant digit.

Analysis of the low-T magnetization series for the (7, 3) lattice, by means of Padé approximants to the logarithmic derivative series, provide estimates for the critical point u_c and the magnetization exponent β. Some of the raw data are shown in table 3. We conclude that $u_c = 0.689 \pm 0.001$ and that $\beta \approx 0.58$, although there is a fair degree of uncertainty in the latter result. Note that $u_c = 0.689$ gives $x_c = 0.184$ and conversely $x_c = 0.1848$ gives $u_c = 0.688$. Thus the critical point estimates from high- and low-T series are quite consistent with each other. The

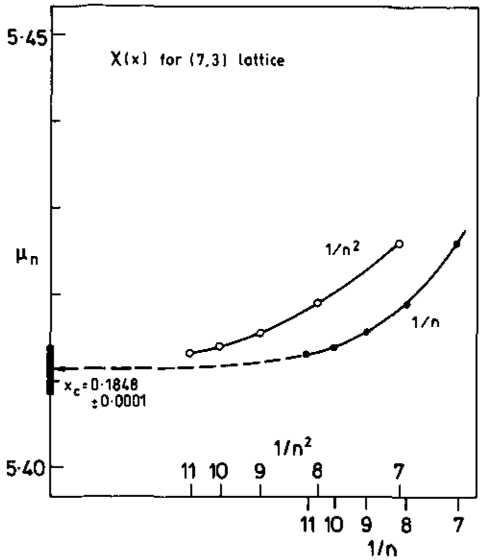

Figure 4. A ratio-plot for the coefficients of the high-temperature susceptibility expansion on the $(7,3)$ lattice.

susceptibility exponent appears to be exactly 1, the classical mean-field value and the value which occurs for infinite effective dimensionality. The corresponding mean-field magnetization exponent would be $1/2$, and our estimate is consistent with this.

Table 3. Estimates of the critical point u_c and exponent β from Padé approximants to the series for $d/du \log M_{\text{fixed}}(u)$, for the $(7,3)$ and $(5,5)$ lattices.

	(7,3)		(5,5)	
$[L/M]$	u_c	β	u_c	β
[13/16]	0.689 98	0.583	0.597 73	0.508
[14/15]	0.689 93	0.582	0.597 70	0.507
[15/14]	0.689 95	0.582	0.597 67	0.506
[16/13]	0.688 81	0.538	0.597 70	0.507
[13/15]	0.689 65	0.570	0.597 65	0.506
[14/14]	0.690 07	0.587	0.597 67	0.506
[15/13]	0.688 62	0.532	0.597 67	0.506

We have analysed the series for the $(5,5)$ lattice in a similar way. The coefficients of the high-T susceptibility series are somewhat more erratic than for the $(7,3)$ lattice. This is consistent with the behaviour found for the usual regular lattices, where higher coordination number generally gives more regular series. The last five ratios μ_n are 3.9702, 3.9680, 3.9680, 3.9683, 3.9681. This suggests that $x_c = 0.2520$ and $\gamma = 1$, again the mean field or infinite-dimensional exponent. Padé approximants to the series for $\chi_{\text{free}}(x)$ and the logarithmic derivative series are consistent with these values and suggest the approximate representation near $x_c = 0.2520$

$$\chi_{\text{free}}(x) = 0.325(x_c - x)^{-1.00} - 0.356 \tag{4.9}$$

where again the estimated errors are ± 1 in the last digits.

Analysis of the low-T magnetization series for the $(5,5)$ lattice by Padé approximants gives the results shown in table 3, from which we estimate that

$u_c = 0.5977 \pm 0.0001$ and $\beta \approx 0.51$. This value of u_c gives $x_c = 0.2518$ and conversely the value $x_c = 0.2520$ gives $u_c = 0.5954$. Again the critical point estimates from high- and low-T series are fully consistent with each other and indicate that the critical exponents have the infinite-dimensional values $\gamma = 1$, $\beta = 1/2$.

The results for the $(5,5)$ lattice are totally unexpected. On the basis of the discussion following (3.18) one would expect that the critical temperatures for the system with free boundary conditions and the system with fixed boundary conditions may well be different but should be related by (3.19). We find something completely different; the critical temperatures are the same for the two boundary conditions (with T_c larger than $T_{\text{self-dual}}$) and the low-T expansion shows no sign of a second critical point at the dual temperature! This is indeed a very strange and unexpected phenomenon. Since the low-T expansions of f_{fixed}, M_{fixed} and χ_{fixed} are all based on the same diagrams they presumably all have the same critical temperature T_c, which happens to be larger than $T_{\text{self-dual}}$. This implies that the high-T expansion of f_{free} has a critical temperature $\tilde{T}_c < T_{\text{self-dual}}$. On the other hand we found that the low-T expansions are regular at $\tilde{T}_c$, so the high-T expansion of f_{free} must be regular at T_c. However, in the high-T expansion of χ_{free}, which is based on a different set of diagrams, we do find a singularity at T_c! This shows that the critical temperatures are independent of the boundary conditions, but do not show up in all thermodynamic functions.

5. Correlation functions at criticality

In the previous section it was found that the susceptibility and the magnetization diverge at a critical temperature. It seems natural that at this critical temperature the Ising model can be described by means of a conformal field theory on the hyperplane. Correlation functions in this conformal field theory can be derived from the corresponding correlation functions in a semi-infinite geometry without curvature by a small extension of the techniques described in [9]. That is done in this section.

Consider a primary field Φ in conformal field theory. Under a conformal coordinate transformation $z \mapsto w = f(z)$ the line element becomes

$$\mathrm{d}s^2 = \mathrm{d}z\,\mathrm{d}\bar{z} = |f'(z)|^{-2}\,\mathrm{d}w\,\mathrm{d}\bar{w} \tag{5.1}$$

and the field transforms as follows

$$\Phi(w,\bar{w}) = f'(z)^{-\Delta}\bar{f}'(\bar{z})^{-\bar{\Delta}}\Phi(z,\bar{z}). \tag{5.2}$$

If we view this mapping as an active mapping between two different geometries with line elements $\mathrm{d}s_1^2 = \mathrm{d}z\,\mathrm{d}\bar{z}$ and $\mathrm{d}s_2^2 = \mathrm{d}w\,\mathrm{d}\bar{w}$ we can relate the correlation functions of primary fields in these geometries:

$$\langle\Phi_1(z_1,\bar{z}_1)\cdots\Phi_n(z_n,\bar{z}_n)\rangle_1 = \prod_{j=1}^{n} f'(z_j)^{\Delta_j}\bar{f}'(\bar{z}_j)^{\bar{\Delta}_j}\cdot\langle\Phi_1(w_1,\bar{w}_1)\cdots\Phi_n(w_n,\bar{w}_n)\rangle_2. \tag{5.3}$$

The line elements of the hyperplane and a (flat) disk are related by rescaling:

$$\mathrm{d}s^2_{\text{disk}} = (1-r^2)^2\,\mathrm{d}s^2_{\text{hyperplane}}. \tag{5.4}$$

There is, however, no holomorphic function $f(z)$ such that

$$(1-r^2)^2 = |f'(z)|^{-2} \tag{5.5}$$

but we do not expect that primary fields for which the two conformal dimensions Δ and $\bar{\Delta}$ are equal can distinguish between rescalings of the metric which are caused by holomorphic coordinate transformations and those which are not.

Therefore we conjecture that the 'critical' correlation functions of spinless (i.e. $\bar{\Delta} = \Delta$) primary fields with scaling dimensions $x_j = \Delta_j + \bar{\Delta}_j$ are

$$\langle \Phi_1(P_1) \cdots \Phi_n(P_n) \rangle_{\text{hyperplane}} = \prod_{j=1}^{n} (1-r_j^2)^{x_j} \cdot \langle \Phi_1(P_1) \cdots \Phi_n(P_n) \rangle_{\text{disk}} . \tag{5.6}$$

This formula will also hold on the hyperlattices if the separations between the points $P_1, \ldots, P_n$ are large.

The correlation functions on the disk can be obtained using standard techniques from conformal field theory [9]. It is convenient to calculate the correlation functions first in the upper-half plane $\mathrm{Im}\, w > 0$ and then transform to the disk via

$$w \mapsto z = \frac{w - \mathrm{i}}{w + \mathrm{i}}. \tag{5.7}$$

For a one-point function with fixed boundary conditions we have on the upper-half plane

$$\langle \Phi(w, \bar{w}) \rangle_{\text{UHP}} = |w - \bar{w}|^{-x} \tag{5.8}$$

hence

$$\begin{aligned} \langle \Phi(z, \bar{z}) \rangle_{\text{disk}} &= \left(\frac{2\mathrm{i}}{(1-z)^2} \right)^{x/2} \left(\frac{-2\mathrm{i}}{(1-\bar{z})^2} \right)^{x/2} \left[\frac{(1-z)(1-\bar{z})}{2(1-z\bar{z})} \right]^{x} \\ &= (1-r^2)^{-x}. \end{aligned} \tag{5.9}$$

Using (5.6) we thus find that the one-point function on the hyperplane is a constant:

$$\langle \Phi(z, \bar{z}) \rangle_{\text{hyperplane}} = 1. \tag{5.10}$$

As a second example we consider the spin–spin correlation function in the Ising model. From [9] we find that on the upper-half plane

$$\langle \sigma(w_1, \bar{w}_1) \sigma(w_2, \bar{w}_2) \rangle \sim \left[\frac{(w_1 - \bar{w}_1)(w_2 - \bar{w}_2)}{(w_1 - w_2)(\bar{w}_1 - \bar{w}_2)(w_1 - \bar{w}_2)(\bar{w}_1 - w_2)} \right]^{1/8} F_{\mp}(\zeta) \tag{5.11}$$

with

$$F_{\mp}(\zeta) = \left\{ \sqrt{\sqrt{1-\zeta} + 1} \mp \sqrt{\sqrt{1-\zeta} - 1} \right\} \tag{5.12}$$

and

$$\zeta = \frac{(w_1 - w_2)(\bar{w}_1 - \bar{w}_2)}{(w_1 - \bar{w}_1)(w_2 - \bar{w}_2)} = -\sinh^2 d \tag{5.13}$$

in terms of the distance $d = d(P_1, P_2)$ between the two points in the hyperbolic geometry. The upper sign is for free boundary conditions, the lower for uniformly fixed boundary conditions. Transforming to the hyperplane we find

$$\langle \sigma(z_1, \bar{z}_1)\sigma(z_2, \bar{z}_2)\rangle_{\text{hyperplane}} = \frac{e^{\mp d/2}}{(e^{2d} - e^{-2d})^{1/4}}. \tag{5.14}$$

From this result we conclude that the correlation function decays exponentially to its asymptotic value:

$$\langle \sigma(z_1, \bar{z}_1)\sigma(z_2, \bar{z}_2)\rangle - \langle \sigma(z_1, \bar{z}_1)\rangle \langle \sigma(z_2, \bar{z}_2)\rangle \underset{d\to\infty}{\sim} e^{-d/\xi} \tag{5.15}$$

where the correlation length is $\xi = 1$ for free boundary conditions and $\xi = 1/4$ for fixed boundary conditions. So even for a massless field the correlations do not have infinite range. This is related to the fact that the spectrum of the Laplacian on the hyperplane has an upper bound of -1 (in our normalization of the metric), whereas the upper bound is zero on the plane; the negative curvature introduces a scale into the problem.

Acknowledgments

Part of this work was financially supported by the Stichting voor Fundamenteel Onderzoek der Materie (FOM).

References

[1] Thompson C J 1982 *J. Stat. Phys.* **27** 441

[2] Saito K 1989 Ising models on Fuchsian groups *Preprint* RIMS

[3] Series C M and Sinai Ya G 1990 *Commun. Math. Phys.* **128** 63–76

[4] Vdovichenko 1965 *Sov. Phys.-JETP* **20** 477
Landau L D and Lifshitz E M A 1980 *Course of Theoretical Physics, vol 5 Statistical Physics* 3rd edn, part 1 (Oxford: Pergamon)

[5] Lund F, Rasetti M and Regge T 1976 *Commun. Math. Phys.* **51** 15

[6] Domb C 1974 *Phase Transitions and Critical Phenomena* vol 3, ed C Domb and M S Green (New York: Academic) p 357

[7] Oitmaa J 1981 *Can. J. Phys.* **59** 15
Oitmaa J and Velgakis M J 1986 *J. Phys. A: Math. Gen.* **19** L553

[8] Guttmann A J 1989 *Phase Transitions and Critical Phenomena* vol 13, ed C Domb and J Lebowitz (New York: Academic) p 1

[9] L Cardy 1987 *Phase Transitions and Critical Phenomena* vol 11, ed C Domb and J Lebowitz (New York: Academic) p 55